Finite-difference time-domain simulation of low-frequency room acoustic problems

D. Botteldooren[a)]
Department of Information Technology, Acoustics Group, University of Gent, 9000 Gent, Belgium

(Received 19 December 1994; revised 12 July 1995; accepted 26 July 1995)

This paper illustrates the use of a numerical time-domain simulation based on the finite-difference time-domain (FDTD) approximation for studying low- and middle-frequency room acoustic problems. As a direct time-domain simulation, suitable for large modeling regions, the technique seems a good ''brute force'' approach for solving room acoustic problems. Some attention is paid in this paper to a few of the key problems involved in applying FDTD: frequency-dependent boundary conditions, non-Cartesian grids, and numerical error. Possible applications are illustrated with an example. An interesting approach lies in using the FDTD simulation to adapt a digital filter to represent the acoustical transfer function from source to observer, as accurately as possible. The approximate digital filter can be used for auralization experiments. © *1995 Acoustical Society of America.*

PACS numbers: 43.55.Ka, 43.55.Fw, 43.60.Gk

INTRODUCTION

In room acoustics, ray tracing is now a well established numerical technique for studying the acoustical quality of a large closed space. However, this approach assumes a frequency that is high enough to allow for geometrical approximations to be applicable. At ultralow frequencies or for small enclosures, a modal approach based on modal profiles calculated in frequency domain, using finite-element or boundary-element numerical techniques, is appropriate in many cases. The middle-frequency range, where a large number of modes are important but where wave behavior still dominates, remains hard to treat. Direct time-domain approaches seem appropriate to solve this problem.

In this paper the numerical approximation used for solving the middle-frequency range problem is the finite-difference time-domain (FDTD) method. This method meets most of the demands required for a good brute force numerical solution of the problem: All calculations are done directly in time domain, acoustical equations are discretized locally resulting in an explicit formulation, and the numerical formulation is itself conservative. A direct calculation in time domain has the advantage of speed, but poses some problems for describing frequency-dependent material characteristics, such as boundary conditions. It will be demonstrated in this paper that this problem is easily solved if the study is limited to a narrow frequency range. A local, explicit formulation is especially useful for large numerical problems since the numerical storage and CPU-time requirements increase only linearly with the number of discretization cells. Also, parallelization of the code for large computers is very easy in this case. Finally, the FDTD numerical approximation used in this paper introduces virtually no numerical error on wave amplitude. The discretization error is mostly a phase error. This feature is very useful for studying long transients in sound-pressure level.

[a)]E-mail: botteldo@intec.rug.ac.be

FDTD simulation is not popular for solving problems in linear acoustics. In contrast, it is one of the very few techniques used to solve (strongly) nonlinear wave equations that govern computational fluid mechanics. The technique is equally popular for electromagnetic-field simulation[1] and for solving optical-field problems.

Lately finite-element (FE) and boundary-element (BE) methods, which were previously used in frequency domain, were also translated to a direct time-domain formulation.[2] It is rather difficult to compare FDTD with these techniques. If it also becomes possible to make the computational effort proportional to the number of discretization cells for these approaches, they become quite competitive. It can be observed that new formulations of FDTD in non-Cartesian grids and closely related finite-volume time-domain simulation tend to become more similar to new finite-element time-domain approaches. The edge between FD and FE is becoming rather vague at this point. As far as BETD techniques are concerned, their biggest disadvantage for the problem at hand is that they are less efficient in information storage than the FDTD method for closed simulation regions. This disadvantage turns into an advantage as the simulation region gets more ''open.''

This paper is organized as follows. First Cartesian FDTD and Voronoi cell FDTD basics are reviewed, paying special attention to numerical accuracy. Then the problem of frequency-dependent boundary conditions is addressed. Finally, the technique is applied for simulating low-frequency room behavior. It will be shown how the simulation method can be used as an addendum to ray tracing for low frequencies and how a low-frequency room evaluation may be conducted.

I. FINITE-DIFFERENCE TIME-DOMAIN SIMULATION

The name of the simulation technique (finite-difference time-domain) for wave propagation problems, used in this paper, refers to the basic formulation. It is essentially based

on a finite-difference approximation for both time and space derivatives in the wave equation. This basic numerical approach is still most efficient in both calculation speed and computer memory requirements. However, since a Cartesian grid is useless for describing non-Cartesian boundary planes, related formulations were developed. In Ref. 3 we describe such a technique, which was named Voronoi cell FDTD (VC-FDTD). It is closely related to numerical approximations, which are sometimes labeled finite-volume time-domain. In this room acoustic study, large central regions are treated by Cartesian FDTD, while VC-FDTD is used to match several regions if necessary.

A. Basic FDTD formulation in a Cartesian grid

The basic formulation of the FDTD approximation uses a Cartesian staggered grid with pressure and particle velocity components as unknown quantities. The acoustical pressure is determined at the grid positions $(i\,\delta x, j\,\delta y, k\,\delta z)$ at time $t = l\ \delta t$, with $\delta x, \delta y, \delta z$ the spatial discretization steps and δt the time discretization step. The indices i, j, k mark the spatial points; the index l marks discrete time. The three components of the particle velocity are determined at positions

$$\begin{aligned} &v_x[(i \pm \tfrac{1}{2})\,\delta x, j\ \delta y, k\ \delta z], \\ &v_y[i\ \delta x, (j \pm \tfrac{1}{2})\,\delta y, k\ \delta z], \\ &v_z[i\ \delta x, j\ \delta y, (k \pm \tfrac{1}{2})\,\delta z], \end{aligned} \tag{1}$$

and at intermediate time $t = (l + \frac{1}{2})\,\delta t$. In this grid the FDTD approximations to the equations of linear acoustics in air become[3]

$$\begin{aligned} v_x^{[l+0.5]}(i+\tfrac{1}{2}, j, k) &= v_x^{[l-0.5]}(i+\tfrac{1}{2}, j, k) - \frac{\delta t}{\rho_0\ \delta x} \\ &\quad \times [p^{[l]}(i+1, j, k) - p^{[l]}(i, j, k)], \\ v_y^{[l+0.5]}(i, j+\tfrac{1}{2}, k) &= v_y^{[l-0.5]}(i, j+\tfrac{1}{2}, k) - \frac{\delta t}{\rho_0\ \delta y} \\ &\quad \times [p^{[l]}(i, j+1, k) - p^{[l]}(i, j, k)], \\ v_z^{[l+0.5]}(i, j, k+\tfrac{1}{2}) &= v_z^{[l-0.5]}(i, j, k+\tfrac{1}{2}) - \frac{\delta t}{\rho_0\ \delta z} \\ &\quad \times [p^{[l]}(i, j, k+1) - p^{[l]}(i, j, k)], \end{aligned} \tag{2}$$

$$\begin{aligned} p^{[l+1]}(i, j, k) &= p^{[l]}(i, j, k) \\ &\quad - \frac{\rho_0 c^2\ \delta t}{\delta x} [v_x^{[l+0.5]}(i+\tfrac{1}{2}, j, k) \\ &\quad - v_x^{[l+0.5]}(i-\tfrac{1}{2}, j, k)] \\ &\quad - \frac{\rho_0 c^2\ \delta t}{\delta y} [v_y^{[l+0.5]}(i, j+\tfrac{1}{2}, k) \\ &\quad - v_y^{[l+0.5]}(i, j-\tfrac{1}{2}, k)] \\ &\quad - \frac{\rho_0 c^2\ \delta t}{\delta z} [v_z^{[l+0.5]}(i, j, k+\tfrac{1}{2}) \\ &\quad - v_z^{[l+0.5]}(i, j, k-\tfrac{1}{2})], \end{aligned}$$

where ρ_0 is the local air density and c is the local speed of sound. Details on the use of this Cartesian FDTD were reported on several occasions. Here only the stability condition, which has to be taken into account when choosing the simulation time step δt, is repeated:

$$c\ \delta t \leqslant \left(\frac{1}{\delta x^2} + \frac{1}{\delta y^2} + \frac{1}{\delta z^2} \right)^{-1/2}. \tag{3}$$

B. Voronoi cell FDTD (finite-volume time-domain)

The Voronoi cell FDTD formulation is based on the integral equations of linear acoustics. It got its name from the choice that was made for the control volumes to which the integral formulation is applied. Around a set of predefined discretization points, the region in simulation space closer to the given point than to other points is constructed. This Voronoi cell is used as control volume for the first integral equation and the first unknown quantity is the average acoustical pressure over this cell. The Voronoi cell is limited by a set of surfaces. It proved useful to define the average orthogonal particle velocity over such a surface as the second unknown quantity and a flat region around the surface as the second control volume. These choices, which introduce a staggeredlike grid, constitute the main difference with known finite-volume time-domain techniques.

The pressure equation that governs the Voronoi cell FDTD is

$$p_i^{[l+1]} = p_i^{[l]} - \frac{\rho_0 c^2\ \delta t}{V_p^{[i]}} \sum_j v_{nj}^{[l+0.5]} S_p^{[j]}, \tag{4}$$

where the summation is over all surfaces that limit the Voronoi cell around point i and $v_{nj}^{[l+0.5]}$ is the average normal particle velocity on surface j at time $t = (l + \frac{1}{2})\,\delta t$. p_i is the acoustic pressure, averaged over the Voronoi cell. The sign of v_{nj} needs special care. The particle velocity v_{nj} is always located exactly in the middle between two pressure points $i-$ and $i+$. Equation (4) assumes v_{nj} has a positive sign if the particle velocity is pointing outward. If this condition is met for point $i-$ the sign in front of v_{nj} in Eq. (4) must be changed for the point $i+$. To solve this problem the convention is introduced that $\mathbf{v}$ on the surface $S_p^{[j]}$ points from the pressure point with lower index $i-$ to the pressure point with higher index $i+$. The appropriate sign can then be introduced in Eq. (4) depending on the order of the set of pressure discretization points. The average particle velocity evolves according to

$$v_{nj}^{[l+0.5]} = v_{nj}^{[l-0.5]} - \frac{\delta t}{\rho_0 d_j} (p_{i+}^{[l]} - p_{i-}^{[l]}), \tag{5}$$

where $p_{i+}^{[l]}(p_{i-}^{[l]})$ is the higher (lower) index nearest-neighbor pressure at time $t = l\,\delta t$ and d_j is the orthogonal distance between the nearest-neighbor volume centers of gravity.

Stability issues are studied in detail in Ref. 3. The Voronoi cell FDTD requires approximately twice as much memory as the Cartesian FDTD and there is a large initial CPU-power consumption. Calculation times during time iterations do not differ substantially from the corresponding Cartesian situation. An interesting increase in accuracy in describing boundaries is possible.[3,4]

C. Numerical error

For the application described in this paper it is important that the numerical technique is conservative. No artificial absorption is allowed. The Cartesian staggered grid formulation, which was described above, fulfills this requirement. Phase error can be tolerated more easily since the major interest is in sound-pressure level which is less sensitive to this type of error.

To study the numerical error, an infinite modeling region is assumed where a plane wave with frequency ω is propagating. The corresponding wave vector is $\mathbf{k}$. First the Cartesian FDTD is considered. Equations (2) are used to express p and $\mathbf{v}$ near a point in space (i,j,k) and in time l as a function of p and $\mathbf{v}$ one time step ago. Unknown pressure at larger distances is calculated, taking into account the spatial behavior of the exact plane-wave solution at $t=(l-1)\,\delta t$. One thus obtains a transfer matrix that relates $p^{[l]}$ and $\mathbf{v}^{[l-0.5]}$ to $p^{[l-1]}$ and $\mathbf{v}^{[l-1.5]}$. The elements of this matrix must be compared to the known exact change of the fields during the time interval δt. After some manipulation, the amplitude of the numerical pressure change is found to be equal to 1, which proves that the FDTD formulation introduces no amplitude error. The numerical phase change during one time step δt, φ_{FDTD}, relates to the exact value φ as

$$\frac{\varphi_{\mathrm{FDTD}}}{\varphi}=\frac{2\ \arcsin\{c\,\delta t\sqrt{\Sigma_\alpha[\sin^2(k_\alpha\delta\alpha/2)/\delta\alpha^2]}\}}{c\,\delta t\sqrt{\Sigma_\alpha k_\alpha^2}}, \tag{6}$$

where the summation is over x, y, and z. It can be seen that it is impossible to choose spatial steps and time steps in such a way that the phase error is zero for all directions of propagation of the plane wave. The error is smallest if the equal sign in Eq. (3) holds and for a propagation direction along the diagonal of the grid cells.

The treatment of the numerical error introduced by the VC-FDTD is much more difficult. The same procedure as described above can still be used. Since the grid is in this case nonuniform, the accuracy depends on the spatial coordinate. For each cell separately, the amplitude error will not necessarily be zero. Since the amplitude error is still expected to be small, the change in the fields during a time step δt is written as $e^{j\omega_{\mathrm{FDTD}}}$, where φ_{FDTD} is a complex number and relates to the exact value φ as

$$\frac{\varphi_{\mathrm{FDTD}}^{[i]}}{\varphi}=\frac{\arcsin\{c\,\delta t\sqrt{\Sigma_j[(S_p^{[j]}/d_j)(1-\beta_{i,j}e^{j\mathbf{k}\cdot(\mathbf{r}_{\mathrm{cg}}^{[i,j]}-\mathbf{r}_{\mathrm{cg}}^{[i]})})]/V_p^{[i]}}\}}{c\,\delta t|\mathbf{k}|}, \tag{7}$$

where

$$\beta_{i,j}=\frac{V_p^{[i]}\int_{V_p^{[i,j]}}e^{-j\mathbf{k}\cdot\mathbf{r}}\,d\mathbf{r}}{V_p^{[i,j]}\int_{V_p^{[i]}}e^{-j\mathbf{k}\cdot\mathbf{r}}\,d\mathbf{r}},$$

where $\mathbf{r}_{\mathrm{cg}}^{[i]}$ is the coordinate of the center of gravity of cell i. The index $[i,j]$ indicates the jth nearest-neighbor cell near cell i. To evaluate Eq. (7), an expansion of the exponential functions is necessary. After some straightforward calculations, it is found that the amplitude error [imaginary part in (7)] is indeed smaller than the phase error and that more symmetrical grids reduce both phase and amplitude error. A more accurate analytical treatment is in this case impossible because errors are often compensated in neighboring cells.

For the application in this paper it is decided from the above considerations to use Cartesian grids in as much of the simulation region as possible.

D. Boundary conditions

Boundary conditions are mostly frequency dependent, even in the relatively small frequency region of interest here. This is an important problem for all time-domain simulations. Taking into account a fully general frequency dependence would require the calculation of a convolution in time domain for each time step and for each boundary point. Since such a calculation is very time consuming it is inadmissible. Good approximations are necessary.

In room acoustics, at low frequencies, two typical absorbing boundary constructions are quite common:
(1) thin (compared to wavelength) absorbing layers on a much harder background, e.g., floor coverings, wall coverings, seats;
(2) light, nonstiff walls and curtains.
The theoretical behavior of the first type of material[5] can roughly be approximated by a complex, frequency-dependent impedance $Z=Z_0+Z_{-1}/j\omega$. The behavior of the second type of material is described quite accurately by $Z=Z_0+j\omega M$, where M is the mass per square meter of the material. Based on these observations it is proposed to approximate a general boundary impedance by

$$Z(\omega)=Z_{-1}/j\omega+Z_0+j\omega Z_1, \tag{8}$$

where Z_1, Z_0, Z_{-1} are real numbers to be determined by fitting experimentally available data and where ω is the pulsation. In fact, Eq. (8) is nothing else than an expansion of $Z(\omega)$ around the frequency of interest, taking into account first-order terms in $j\omega$ and $(j\omega)^{-1}$. In time domain, the impedance in Eq. (8) leads to the boundary condition

$$p(t)=Z_{-1}\int_{-\infty}^{t}v_n(\tau)d\tau+Z_0v_n(t)+Z_1\frac{dv_n(t)}{dt}, \tag{9}$$

where $p(t)$ is the acoustic pressure and $v_n(t)$ is the component of particle velocity orthogonal to the boundary plane.

Alternatively, the boundary construction itself can be modeled using FDTD simulation. Research was conducted along these lines and some results were reported in Ref. 6. The results are not very different from results obtained using boundary impedance. The approach will not be expanded in this paper.

The boundary condition in Eq. (9) proves to be a good starting point to derive an FDTD boundary condition. For simplicity the equations are only derived here for a Cartesian implementation, where the boundary is at a plane $z=(k_0+0.5)dz$ and where the modeled region is at lower z values. The boundary condition is implemented at a velocity plane. Equation (2) cannot be used to determine the normal particle velocity v_z at the boundary since $p(i,j,k_0+1)$ is not

known. To solve the problem an asymmetric finite-difference approximation for the space derivative is introduced:

$$\left.\frac{\partial p}{\partial z}\right|^{[l]}(i,j,k_0+\tfrac{1}{2})=\frac{2}{\delta z}\,[p^{[l]}(i,j,k_0+\tfrac{1}{2})-p^{[l]}(i,j,k_0)]. \tag{10}$$

Although this asymmetric form is only accurate to within δz (δz^2 for the symmetric form), it has the advantage over a second-order FD approximation near the boundary, that it requires only the knowledge of one nearest pressure. $p(i,j,k_0+0.5)$ is not known, but Eq. (9) can be used to write it as a function of v_z. This results in a boundary cell FDTD equation:

$$\begin{aligned}
&v_z^{[l+0.5]}(i,j,k_0+\tfrac{1}{2})\\
&\quad=v_z^{[l-0.5]}(i,j,k_0+\tfrac{1}{2})\\
&\qquad-\frac{2\,\delta t}{\rho_0\delta z}\Bigg[-p^{[l]}(i,j,k_0)+Z_0 v_z^{[l]}(i,j,k_0+\tfrac{1}{2})\\
&\qquad+Z_1\,\frac{v_z^{[l+0.5]}(i,j,k_0+\tfrac{1}{2})-v_z^{[l-0.5]}(i,j,k_0+\tfrac{1}{2})}{\delta t}\\
&\qquad+Z_{-1}\,\delta t\sum_{m=-\infty}^{l} v_z^{[m-0.5]}(i,j,k_0+\tfrac{1}{2})\Bigg],
\end{aligned} \tag{11}$$

where the finite-difference approximation was introduced for the time derivatives and the integration is replaced by a summation. The only unknown variable in Eq. (11) is the particle velocity v_z at $t=l\ \delta t$. A linear interpolation is used to express it as a function of v_z at $t=(l-0.5)\delta t$ and $t=(l+0.5)\delta t$, which are the unknown quantities. Now the equation can be solved for $v_z^{[l+0.5]}$ as a function of previous values of v_z and the nearby pressure $p(i,j,k_0)$:

$$\begin{aligned}
&v_z^{[l+0.5]}(i,j,k_0+\tfrac{1}{2})\\
&\quad=\alpha v_z^{[l-0.5]}(i,j,k_0+\tfrac{1}{2})+\beta\,\frac{2\ \delta t}{\rho_0\ \delta z}\Bigg[p^{[l]}(i,j,k_0)\\
&\qquad-Z_{-1}\delta t\sum_{m=-\infty}^{l} v_z^{[m-0.5]}(i,j,k_0+\tfrac{1}{2})\Bigg],
\end{aligned}$$

with

$$\begin{aligned}
\alpha&=\frac{1-Z_0/Z_{\mathrm{FDTD}}+2Z_1/Z_{\mathrm{FDTD}}\delta t}{1+Z_0/Z_{\mathrm{FDTD}}+2Z_1/Z_{\mathrm{FDTD}}\delta t},\\
\beta&=\frac{1}{1+Z_0/Z_{\mathrm{FDTD}}+2Z_1/Z_{\mathrm{FDTD}}\delta t},\\
Z_{\mathrm{FDTD}}&=\frac{\rho_0\ \delta z}{\delta t}.
\end{aligned} \tag{12}$$

The appropriate equation in the set of equations (2) can be replaced by Eq. (12) at the boundary. To calculate the summation in Eq. (12), one new variable, where the sum "up to now" is stored, is necessary for the boundary cells.

Since the discretized equations used near boundaries are applied in very different contexts (e.g., on flat walls, in corners, close to other boundary conditions) it is not possible to treat stability in general. Only some sufficient conditions for stability are given. Less severe conditions normally result in stable simulations as well. It can be shown that stability is guaranteed for all positive values of Z_0 and Z_1 and all simulation regions if

$$c\ \delta t\leqslant\sqrt{\frac{2}{3}}\left(\frac{1}{\delta x^2}+\frac{1}{\delta y^2}+\frac{1}{\delta z^2}\right)^{-1/2}. \tag{13}$$

In practical situations condition (3) is, however, mostly sufficient. If Z_{-1} is nonzero, stable FDTD simulation is only possible for δt that meet

$$c\ \delta t\leqslant\delta z\left(\frac{1+2Z_1/\rho_0\delta z}{1+Z_{-1}\delta z/\rho_0 c^2}\right)^{1/2} \tag{14}$$

if the boundary is orthogonal to the z direction. This condition is more severe than Eq. (3) if Z_{-1} is large compared to $\rho_0 c^2/\delta z$.

E. Digital electronics simulation

Time-domain simulations, just as experimental sound registrations, contain a lot of information. However, this information is hard to manage in its raw form. Therefore some signal processing is necessary. For the applications described in this paper, digital signal processing capabilities are incorporated in the simulator. The DSP library includes adders, multipliers, FIR and IIR filters, rectifiers, integrators, signal generators, etc. For the evaluation of transient signals, 1/1-octave- and 1/3-octave-band filters are used frequently as well as sound-pressure level calculators. The band filters are 12th-order Butterworth filters, implemented in six IIR stages. The octave-band filters are in compliance with international standards. The sound-pressure level calculators include linear and exponential averaging. The time constant τ_{av} of the exponential averaging is an important parameter for the transient results given in this paper. Room quality descriptors such as Deutlichkeit and Clarity are implemented as well, although their use for low-frequency evaluation is doubtful. The digital signal processing time step can be any integer multiple of the FDTD time step δt.

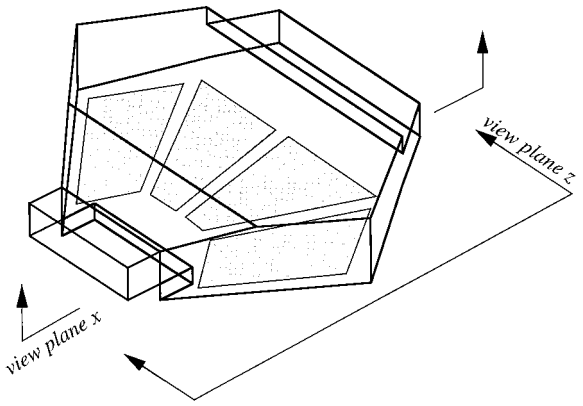

FIG. 1. Schematic view of the auditorium that is modeled as an example, indicating the two observation planes.

TABLE I. Sabine absorption coefficients of materials in the room.

f (Hz)	Parquet	Persons	Curtain	Plaster	Carpet
63	0.03	0.16	0.05	0.02	0.02
125	0.04	0.17	0.05	0.03	0.02
250	0.04	0.24	0.03	0.05	0.06
500	0.05	0.56	0.035	0.04	0.13

II. LOW-FREQUENCY RESPONSE OF A ROOM

A. Description of the example

In this section the possibilities of FDTD simulation for studying the low-frequency acoustical behavior of rooms are illustrated. The layout of the multifunctional room is shown in Fig. 1. Table I gives the absorption coefficients for the material surfaces that are used in the room. The frequency-dependent boundary conditions are approximated by fitting an acoustical impedance of the form (8) on the data from Table I. The resulting Z_{-1}, Z_0, and Z_1 are given in Table II. The simulation region is discretized using a rough and a fine grid. The rough grid consists of 27 750 cells with an average diameter of 50 cm; the fine grid has 232 560 cells with average dimensions of 25 cm. It is known from experience that the first grid allows reasonably accurate simulations for frequencies up to about 70 Hz, while the second grid is useful for studying acoustic fields containing frequencies below about 140 Hz. The time step δt is equal to 0.5 ms for the first grid and 0.25 ms for the second grid.

B. Reverberation (impulse response)

A traditional method for a first evaluation of the acoustic quality of a room consists in measuring the reverberation or impulse response of the room at different locations. The same evaluation can be performed directly using the FDTD simulation. A loudspeaker is modeled in the front of the room. The membrane velocity is an impulselike function of time:

$$v(t)=(t-t_0)\exp(-(t-t_0)^2/\sigma), \tag{15}$$

where the choice of the Gaussian width σ determines the range of frequencies excited. This range should always be well below the accuracy limit imposed by the discretization step. The excitation of Eq. (15) was found to be very useful for FDTD simulations.

During the simulation the sound pressure is recorded at the places of interest. To reduce storage space and output operations to disk, the pressure is directly fed to appropriate octave-band filters and rectified to obtain a sound-pressure level in dB. The time constant τ_{av} of the exponential averaging is equal to 1/32 s.

TABLE II. Impedance approximations for materials in the room.

	Parquet	Persons	Curtain	Plaster	Carpet
Z_1	6.0	0.0	5.0	6.0	0.0
Z_0 ($\times 10^3$)	20.0	4.3	15.5	15.0	40.6
Z_{-1} ($\times 10^6$)	8.0	0.8	0.0	16.0	0.0

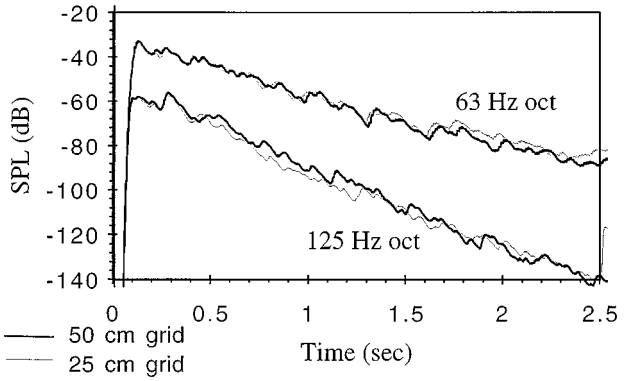

FIG. 2. Transient sound-pressure level (SPL) in the center of the auditorium calculated with grid steps of 50 (thick line) and 25 cm (thin line).

To get a general idea about the accuracy of the simulation in real situations, the impulse response at a point in the center of the room is calculated using both grids and is compared in Fig. 2. For the 63-Hz octave band, results of both simulations correspond quite well. The small differences in detailed behavior after long simulation times are due to the phase error. For the 125-Hz octave band, differences are larger as could be expected from the easy rule of thumb that the spatial grid step must be about one-tenth of the relevant wavelength in the sound, a condition that is not fulfilled for the rough grid.

As an example, Fig. 3 compares the impulse response in the middle of the room, in front, to the response in a corner at the back. Using good visualization software, the impulse can also be followed in its propagation through the room.

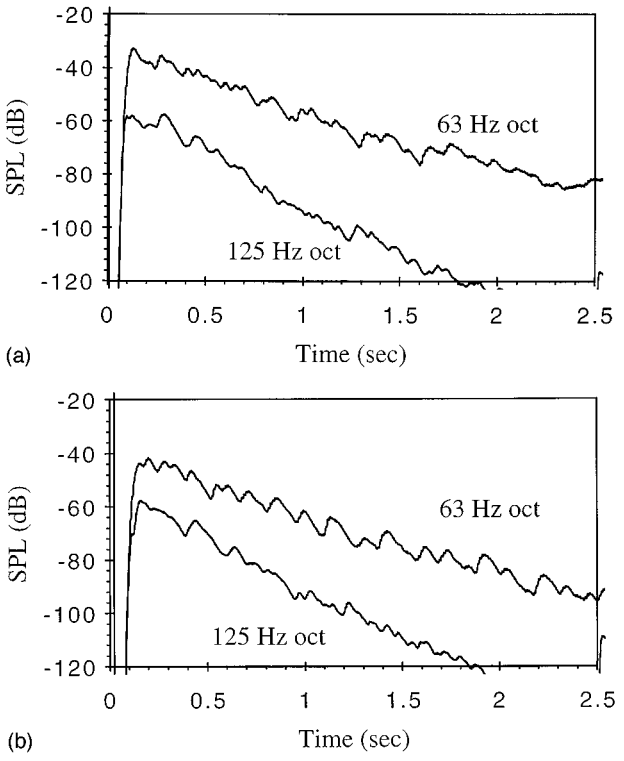

FIG. 3. Transient SPL in (a) the front center of the auditorium and (b) in a back corner. Pulse excitation and postfiltering in 63- and 125-Hz octave bands.

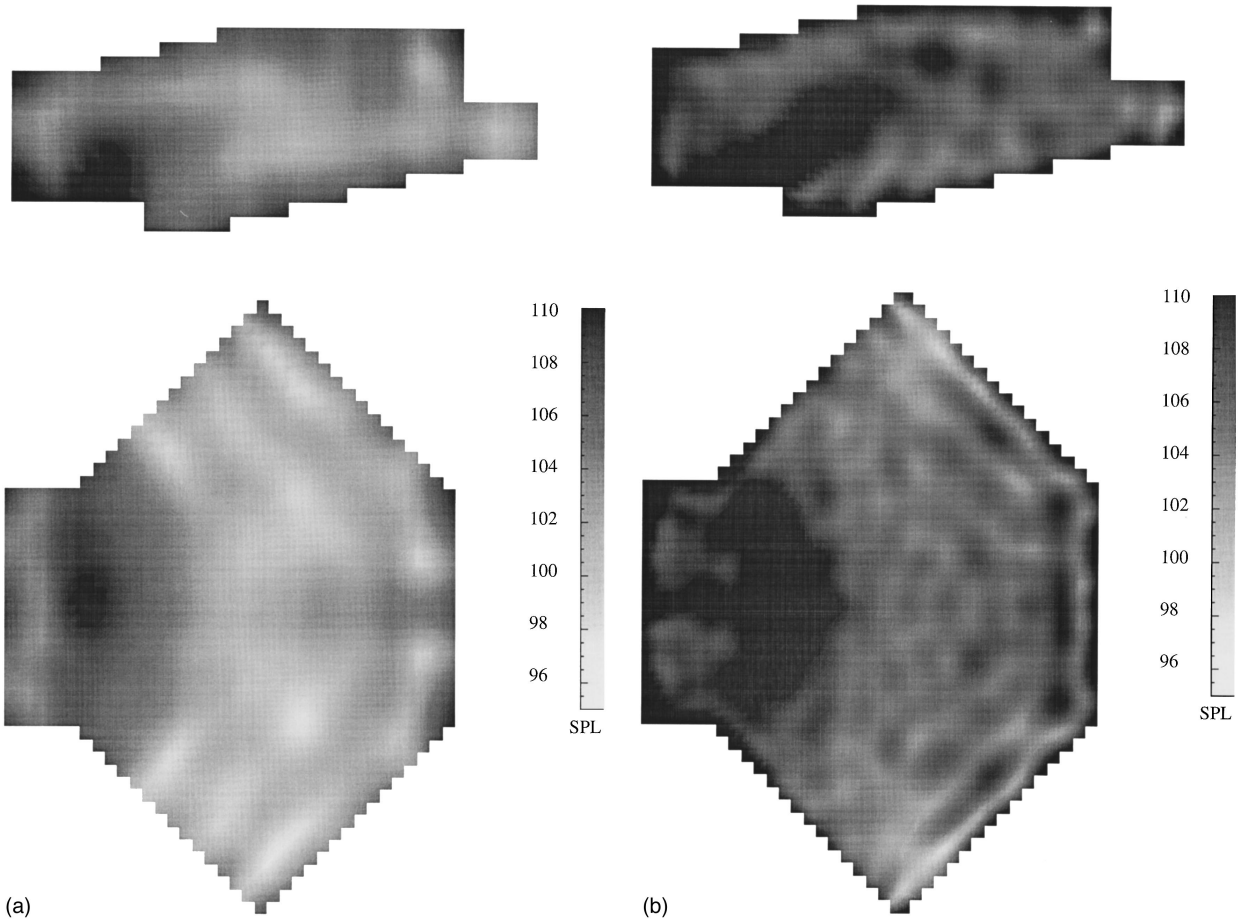

FIG. 4. Sound-pressure level distribution in the room for excitation by octave-band filtered white noise; (a) 63- and (b) 125-Hz octave band.

This exercise allows the designer to get a good feeling of what is happening.

C. Response for specific signals

At the low frequencies considered here, the evaluation of the acoustic quality of a room remains a difficult task. In principle the time-domain model used in this paper allows one to simulate the response of the room to whichever input signal is desired. To cover the full frequency range of interest, other techniques such as ray tracing must be used to obtain the response at higher frequencies. To illustrate the possibilities of the model, two aspects of the problem are studied in detail: the spatial distribution of sound-pressure levels for the low-frequency components in a sound and the response for an observer at a specific place in the room.

Spatial sound-pressure level distributions can be calculated in frequency domain. However, pure tones with long duration are quite uncommon in music. Treating the uniformity problem for specific frequencies therefore tends to exaggerate the sound-pressure spatial nonuniformity in comparison to what is observed for real music. A valid alternative could be to calculate sound-pressure level distributions for sine signals of finite length, special bandlimited impulses, or bandlimited noise. As an example, Fig. 4 shows sound-pressure level distributions (L_{eq}) in the vertical and the horizontal plane marked in Fig. 1 for an excitation that is generated by filtering white noise through a 63- or a 125-Hz octave-band filter, respectively. The integration time for calculating the L_{eq} is chosen to assure that further simulation does not change the resulting spatial distribution a lot. Observe the standing-wave pattern for the 63-Hz octave-band excitation and the more pronounced wave behavior near boundaries for the 125-Hz octave-band excitation.

A possible approach to evaluate the acoustical quality of a listening environment is to filter a sound by the expected characteristic of the listening room and then feed the result to a headphone or an anechoic test environment. At low frequencies one could try to feed the sound to the FDTD simulation to obtain the expected sound near one of the seats in the auditory. However, for the 125-Hz simulation, a modern workstation takes about 60 min to simulate 1 s of sound. This is clearly not a real-time simulation. Even if the calculation is performed off line, simulating 1 min of music (only the low-frequency part) would take several days. Therefore an approximate technique is suggested in the next paragraph.

D. Approximate digital filter

For auralization, real-time simulation of the acoustical transfer function between the source and the listener is required. Since the FDTD simulation is itself too slow to perform this task, it is proposed to find a digital filter that ap-

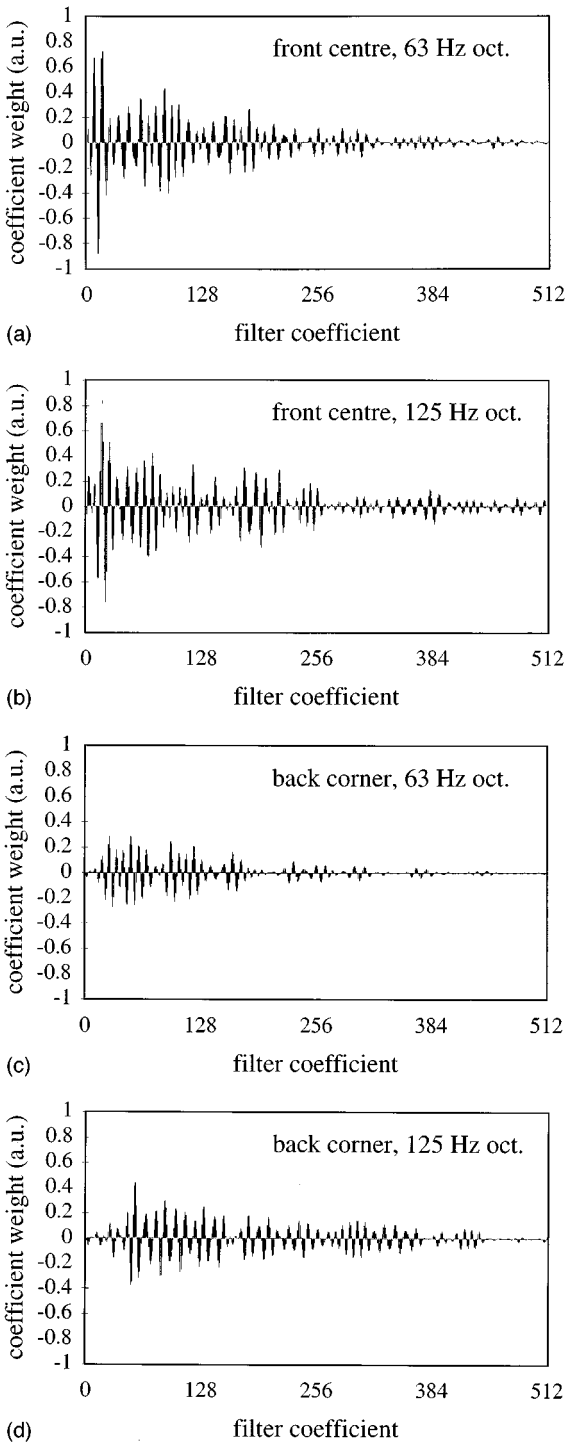

FIG. 5. FIR filters (first 512 coefficients from 2048) approximating the room transfer functions (a) to the front center for 63-Hz octave-band noise, (b) to the front center for 125-Hz octave-band noise, (c) to a back corner for 63-Hz octave-band noise, and (d) to a back corner for 125-Hz octave-band noise.

proximates the acoustical transfer function relatively well and use DSP processors to implement this filter.

Two methods can be used to find the digital filter that approximates the acoustical transfer function. The first method consists in obtaining the transfer function in frequency domain from the FDTD simulation by Fourier transformation of a simulated impulse response and then approximating this desired filter characteristic using well established filter design methods. The second approach consists in finding the FIR-filter coefficients directly by using adaptive methods to minimize the difference between the filter output and the output of a microphone in the FDTD simulation. Well established techniques, such as the LMS algorithm,[7] can be used for this purpose. In this paper the adaptive filter method is used. The probing sound is again octave-band filtered white noise. The resulting FIR filter can be used as part of a parallel bench of octave-band filters followed by transfer function filters, which are obtained here for low frequencies and which are calculated by well-known ray tracing techniques for high frequencies. FIR filters with 1024 or 2048 tabs perform quite well. After convergence of the adaptive algorithm, the difference between the output of the filter and the simulated microphone signal is typically 30 dB below the sound-pressure level. The first 512 filter coefficients for the 63- and the 125-Hz transfer function FIR filters are shown in Fig. 5 for acoustical response at two positions in the room. The sampling step is 2 ms for the 63-Hz filters and 1 ms for the 125-Hz filters.

III. CONCLUSIONS

In this paper it is demonstrated that a finite-difference time-domain approximation is useful for simulating the acoustical behavior of rooms at low frequencies. Using a time-domain technique corresponds quite well to the special interest that the room acoustician has in time domain. Using FDTD seems to have an advantage over other techniques when large problem spaces are treated, which is clearly the case in the application described in this paper. To be able to apply the technique, an efficient approximation for frequency-dependent boundary conditions and an FDTD formulation in nonorthogonal grids are combined. Some examples of possible uses of the simulation are given, focusing especially on evaluation by listening to filtered sounds.

ACKNOWLEDGEMENT

Dr. ir. D. Botteldooren is a senior research assistant with the Belgian National Fund (NFWO) for Scientific Research.

[1] K. S. Kunz and R. J. Luebbers, *The Finite Difference Time Domain Method for Electromagnetics* (CRC, Boca Raton, FL, 1993).
[2] J. P. Coyette, "Transient acoustics: evaluation of finite element and boundary element methods," Proceedings of ISMA 19, Leuven, Belgium, 1994, pp. 223–234.
[3] D. Botteldooren, "Acoustical Finite Difference Time Domain Simulation in a Quasi-Cartesian Grid," J. Acoust. Soc. Am. **95**, 2313–2319 (1994).
[4] D. Botteldooren and H. Devos, "Non-uniform Grids for Acoustical FDTD-Simulations," Proceedings of the Third International Congress on Air- and Structure-borne Sound and Vibration, Montreal, Canada, 1994, pp. 849–856.
[5] L. L. Beranek and I. L. Vér, *Noise and Vibration Control Engineering* (Wiley, New York, 1992).
[6] D. Botteldooren, "Finite Difference Time Domain Study of Acoustical Cavities with Vibrating Plate Boundaries," Proceedings of Internoise 93, Leuven, Belgium, 1993, pp. 1577–1581.
[7] S. Haykin, *Adaptive Filter Theory* (Prentice-Hall, Englewood Cliffs, NJ, 1991).